BELARUSIAN STATE UNIVERSITY

Automation of CMS Phase II Tracker Module assembly

by

Artsiom Bryksa

A thesis submitted in fulfillment for the
degree of Specialist

in the

Faculty of Radiophysics and Computer Technologies
Department of Telecommunication and Information Technologies

March 2017

BELARUSIAN STATE UNIVERSITY

Abstract

Faculty of Radiophysics and Computer Technologies
Department of Telecommunication and Information Technologies

by Artsiom Bryksa

The CMS phase II upgrade outer tracker is built from two types of modules (PS and 2S) each consisting of two silicon sensors and associated electronics and mechanics. In the case of the PS module, the sensors has be assembled to a precision of approximately 40 mm. In order to satisfy this requirement and a short module assembly time, an automated assembly system is proposed. This systems based on a high-precision motion-stage integrated with high-resolution camera, which provides pattern-recognition, vacuum holding system and control systems. [1]

Acknowledgements

James Keaveney, Andreas Mussgiller, Doris Eckstein, Carsten Muhl, Adam Zuber and all the CMS group in DESY for being ready to help anytime I had questions, while I had lots of them...

Contents

Abbreviations

CMS	**C**ompact **M**uon **S**olenoid
LHC	**L**arge **H**adron **C**ollider
...	

Chapter 1

Introduction

The Large Hadron Collider (LHC) is the largest particle accelerator in the world. During the first run of it from 2010 to 2013 its experiments had made remarkable achievements. Perhaps one of the most famous is the discovery of the theorised Higgs particle, which resulted in the Nobel Prize in Physics in 2013 being awarded to Franois Englert and Peter Higgs. The LHC are made to collide particles at four locations around the accelerator ring, corresponding to the positions of four particle detectors ATLAS, CMS, ALICE and LHCb [2].

1.1 Compact Muon Solenoid

The Compact Muon Solenoid (CMS) is a cylindrical particle detector designed to measure a wide range of particles produced in the collisions of LHC. The size of the detector is around 28 m long and 15 m in diameter. It is the heaviest detector in the world and weighs approximately 14000 t. The name "CMS" originates from the three key characteristics of the detector: its relatively compact size, its excellent capabilities in the detection and measurement of muons and its central feature, a superconducting 3.8T solenoid magnet.
The CMS detector consists of many separate detector layers, each of them playing an individual role in detecting and measuring the traversing particles. A cross-sectional overview of the layers and its tasks in reconstructing tracks of particles is shown in the Figure 1.1.

1.2 Phase II Upgrade of CMS Tracker

After Phase II Upgrade, the LHC will provide a much higher luminosity. This regime is known as the High Luminosity LHC (HL-LHC). A serious problem presented by these

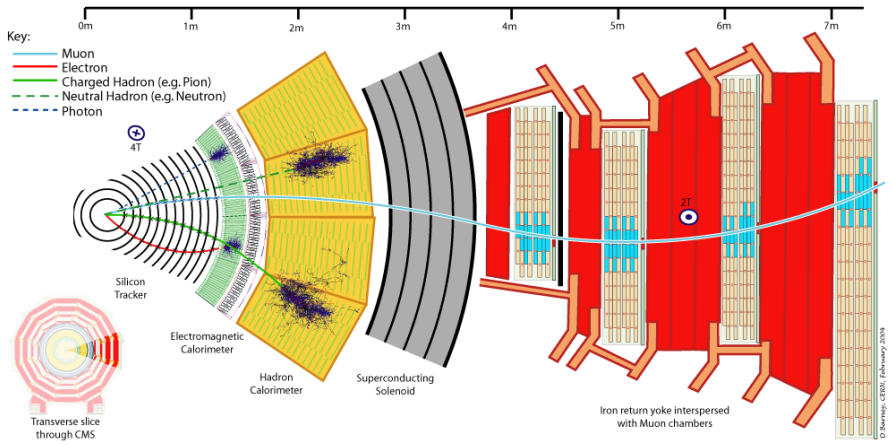

FIGURE 1.1: A cross-sectional view of the CMS detection layers.

conditions is the enormous data readout rates that exceed far beyond the bandwidth foreseen for the readout electronics [2]. However, the vast majority particles produced in the HL-LHC conditions are not of direct interest for new physics searches and are characterized by low transverse momentum. Thus rejecting tracker hits related to low transverse momentum particles can significantly reduce the amount of data to be read-out. In order to provide momentum discrimination at the hardware level, a 2-layer module design was created. The central idea of the new modules is to provide fast discrimination between low and high momentum particles by estimating the track curvature caused by the magnetic field within the volume of the module itself. For example, particle with high transverse momentum after hitting some pixel/strip at the first sensor layer would hit on of neighboring pixels/strips of the respective pixel/strip on the second layer. While a particle with low transverse momentum would have a more curved trajectory an hit pixel/strips at a displaced position from the first hit. By varying the distance between sensors and number of neighboring pixel/strips required to match hits in adjacent sensors, (2 neighboring strips in the Figure 1.2) it is possible to set the transverse momentum threshold for a hit.

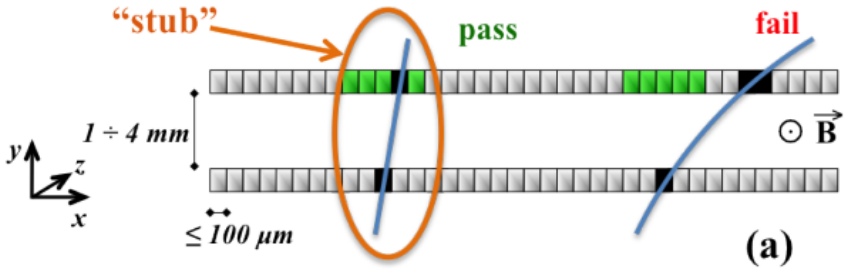

FIGURE 1.2: An example of distinguishing high and low transverse momentum. Particles, which hit any of two neighboring strips or the respective strip itself, would be record as high transverse momentum particles.

1.2.1 Two layer Modules

The CMS Phase-II Tracker will utilize two types of modules, 2S modules and PS modules. To achieve efficient rejection of low-pT particles throughout the Tracker volume, modules in different regions will make use of a few different sensor spacings. For 2S (PS) modules, spacings of 1.8 and 4 mm (1.6, 2.6 and 4 mm) are foreseen. These modules will be used in the end-cap disks as well as the central barrel region of the Tracker. An exploded view of a PS module is shown in Figure 1.3. In the PS module, the sensors are glued to a carbon-fibre reinforced Aluminium (AL-CF) spacers which act as spacers and provide the thermal conductance crucial for the cooling of the module. The two sensors and spacers are in turn glued the carbon-fibre (CF) baseplate. This structure is henceforth referred to as the sensor-spacer-baseplate-assembly (SSBA). This project will focus on the assembly of the SSBA only. The precision requirements of the SSBA are shown in figure ??. For the PS module, the sensors must align to within 40 mm measured at the sensors short edge. This corresponds to a rotational alignment tolerance of 0.8 mrad.

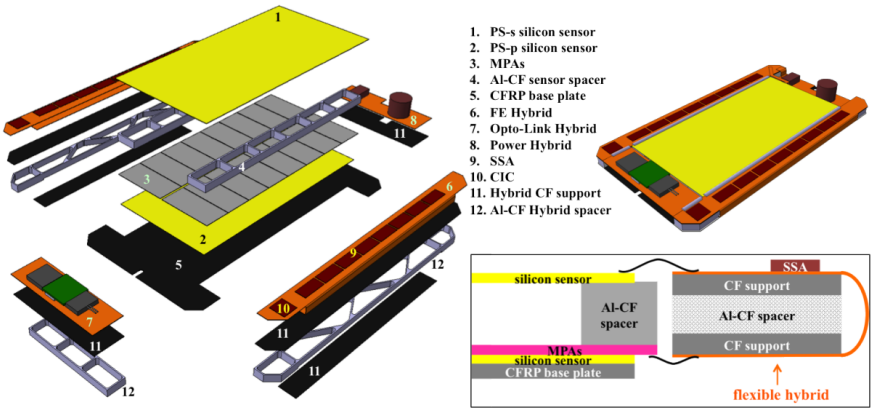

FIGURE 1.3: Exploaded view of Pixesl Sensor Module.

1.2.2 Assembly of two layer sensors

Chapter 2

Modules assembly

[Advantages and disadvantages of automated and manual assembly. Automated assembly is the best!!!]

2.1 Automated assembly steps

[Perhaps I should put this section later...?] Steps [list]: 1) Spacers to platform 2) Glue upper sensor to spacers 3) Rotate 90 degrees 4) Remove spacer+upper sensor 5) Put baseplate on the assembly platform 6) Glue bottom sensor (bare module) to the baseplate 7) Glue Upper sandwitch to the bottom one.

2.2 Assembly platform

2.2.1 Requirements for assembly platform

2.2.2 Design

2.3 Fast adhesive

Chapter 3

Automated assembly...

3.1 Section 1

Chapter 4

Fast adhesive

4.1 Fast glue implementation options

4.2 Candidates

4.3 Tests

4.4 Glue joint thickness

4.5 Fast glue conclusions

Chapter 5

Precision estimation tests

The automated assembly system has a number of properties in terms of precision:

1. Motion stage movement repeatability.
2. Image acquiring repeatability.
3. Precision of pattern recognition.
4. Possible movements of a sensor while picking them up and down with the vacuum pick up tool.
5. ...

In order to investigate this properties a series of tests were done.
Real sensors will be very thin (around 200 um). This fact makes them very fragile. Even though dummy sensors, which will be used for further experiments, is a bit thicker (around 300 um), they are still too fragile for the first tests, because the bottom surface of the pick up tool and the plane underneath testing samples are not yet parallel enough. That is why for the first pick up and down tests we used glass samples. They have the same dimentions and represent close enough the properties of silicon sensors. Moreover, they are much cheaper, so that in case of test failure (sample breakes) it will not be such a big problem as if silicon sample crashes. Despite all mentioned above, none of glass samples where crashed.
Even though we did not do the pick up test with silicon samples, there is still an opportunity to get some information of the pick up and down precision of the silicon samples without direct testing of them [?]. By making a full range of tests with glass samples, we will be able to say how pick up and down influences the precision. Based on this results we will be able to approximately predict the precision of pick up and down tests with silicon samples. Later, when parallelness of the bottom surface of the pick up tool and samples will be provided, we will be able to confirm the results of

the prediction. More information concerning precision of pick up and down of silicon samples one can see in the section XX.

5.1 Pattern recognition precision tests

For investigation of the pattern recognition precision the folowing tests were done. During these tests samples were not moved, so that the additional errors by vacuum pick up and down can be excluded.

5.1.1 Pattern recognition on the painted corner of a glass dummy

In the very first test we investigated the pattern recognition on the corner of the sample. Thin pieces of glass with a silver painted corner (Figure 5.1) were used for the tests as an approximation of a silicon sensor.

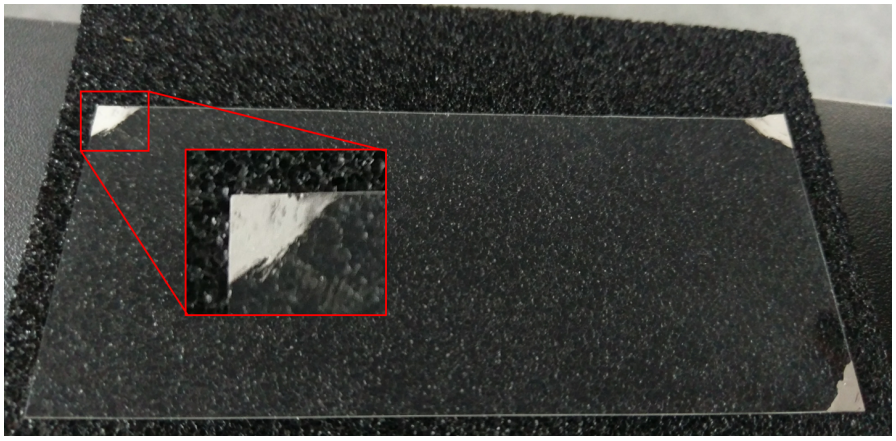

FIGURE 5.1: Glass sample with silver painted corner.

The step-by-step outline of this test is listed below:

1. Move to the image acquiring position.
2. Acquire image and run pattern recognition.
3. Move aside for 5 mm in all axes (?).
4. Move to the image acquiring position.
5. Acquire image and run pattern recognition.
6. Save data of the current iteration and go to the next one.

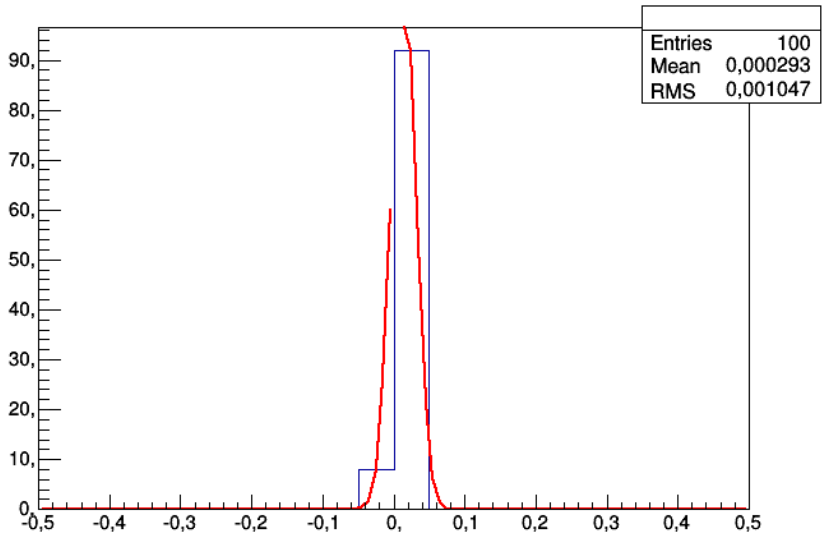

FIGURE 5.2: Distribution of the differnece between detected X coordinate of the master image before and after moving the arm in each iteration.

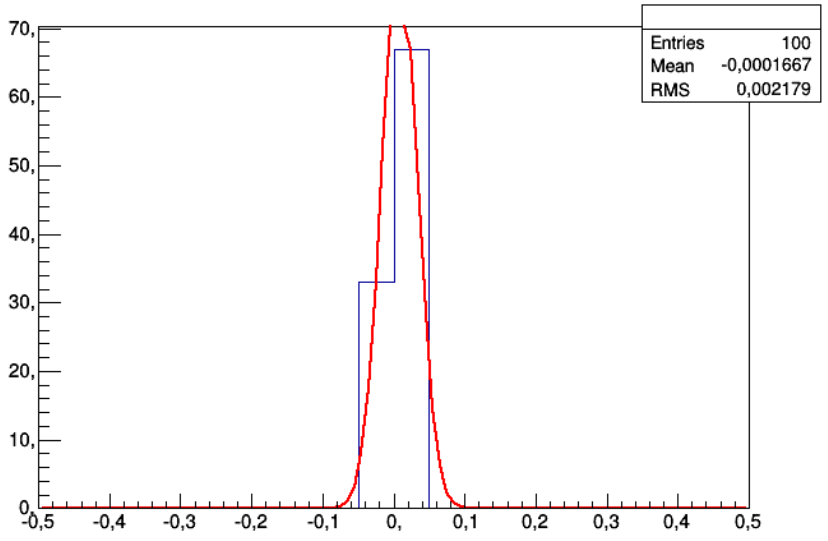

FIGURE 5.3: Distribution of the differnece between detected Y coordinate of the master image before and after moving the arm in each iteration.

After each step software saves the difference between measured cordinates before and after moving the arm with the camera. The distributions of these values are showed in Figure 5.2, Figure 5.3 and Figure 5.4. The test had 100 iterations done in a row.

Looking at the Figures 5.2 and 5.3 one can see that the X, Y detection of the pattern recognition has enough good precision (1-2 um of error [?]), while the theta detection results do not look so precise. There are several reasons of such behavior. The main one them is shown on the Figure 5.5.

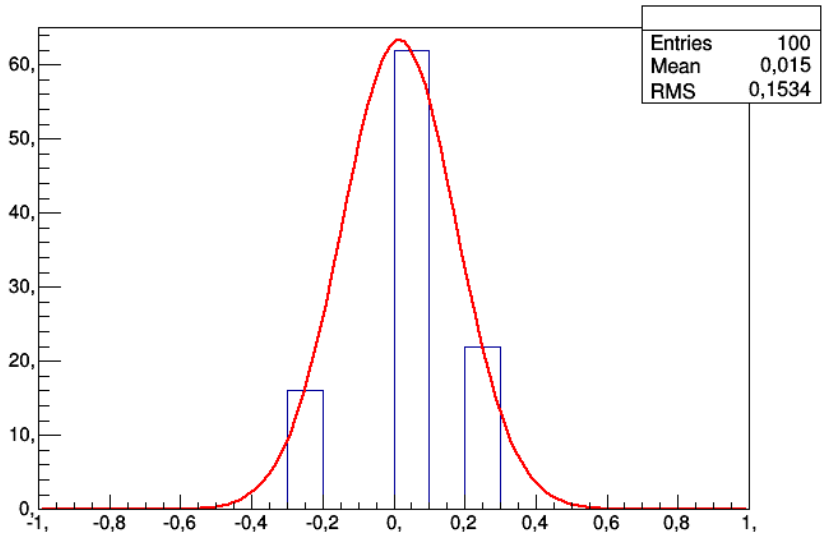

FIGURE 5.4: Distribution of the differnece between detected angle orientation of the master image relaticely to the acquired image before and after moving the arm in each iteration.

Silver painted surface is not flat in 100 um scale. Due to this roughness different amount of light reflects to the camera from different points along the paint surface. That is why the painted corner contains various shades of grey, which [?] in some points are darker, than the table underneath the sample (background). All these result into the picture one can see in the Figure 5.5. This kind of pictures has random distribution of dark areas on it. That is why the pattern recognition algorithm has such error while comparing two pictures (master template and acquired image) with random distribution of black areas. Moreover, this kind of tests lasts around one hour, which is long enough for the sun light to change its luminosity. Even though all reasonably possible measures were done to prevent such effect, the acuired image is very sensetive for light. For example, the effect of the sunny light can results in the threshold variation for 20 units (the color depth is 256) even with closed jalousie. [should I mention it...?]

5.1.2 Pattern recognition on the marker of the dummy sensor

The same test, but with dummy silicon sensor and real marker on it, was done. Before the test marker was aligned as much close to zero degrees as possible. At the Figure 5.6 one can see that the edge of the marker after applying Threshold is almost perfect (+/- one pixel). This fact itself is already a proof that Threashold step of pattern recognition is feasible.

The Distribution of X and Y coordinates are shown on the Figure XX The results of the test is shown on the Figure ...

FIGURE 5.5: The view of the corner after applying the Threshold.

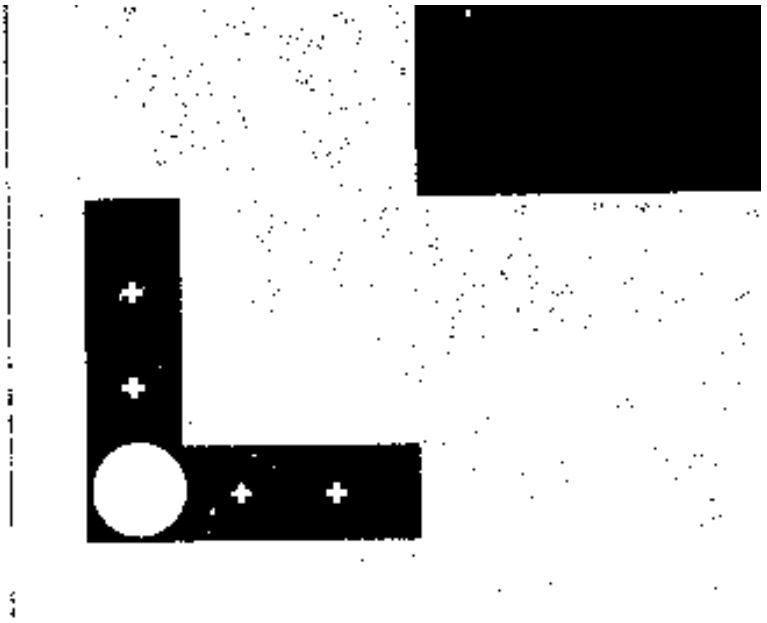

FIGURE 5.6: Sensor marker after applying Threshold.

A screenshot of the application during the test is shown on the Figure 5.7. On the pattern recognition curve one can see that exactly at 0 degree there is a underlinefluctuation (a short upward shot) (?).

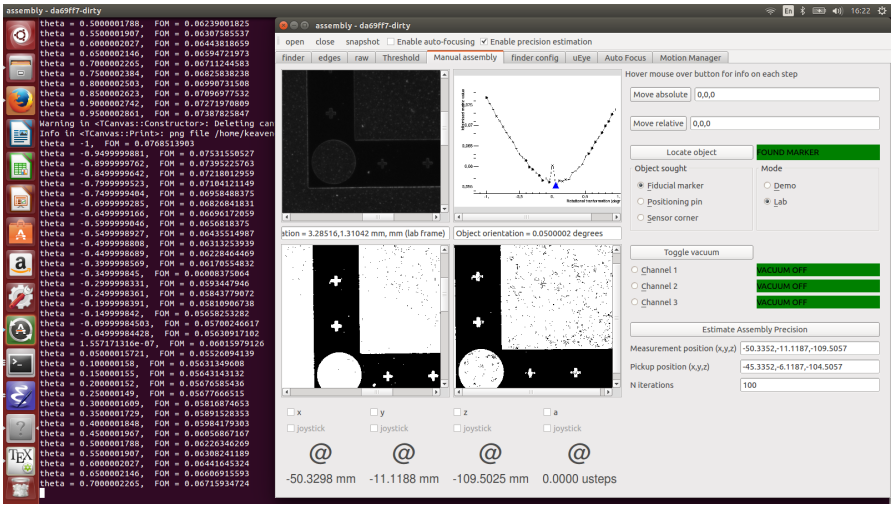

FIGURE 5.7: Screenshot of application during precision extimation test with dummy silicon sensor and marker on it.

5.2 Vaccuum pick-up and -down precision

0) Move to measurement position 1) Corner position 2) Move to pre-pickup position (!) 3) Move to pickup 4) Toggle vacuum 5) Move up 6) Move down 7) Release vacuum 8) Move to pre-pick-up 9) Move to measurement position 10) Corner position

Chapter 6

Conclusion

6.1 Results

6.2 Future plans

Bibliography

[1] C. J. Hawthorn, K. P. Weber, and R. E. Scholten, "Littrow configuration tunable external cavity diode laser with fixed direction output beam," *Review of Scientific Instruments*, vol. 72, pp. 4477–4479, December 2001.

[2] C. J. Hawthorn, K. P. Weber, and R. E. Scholten, "Littrow configuration tunable external cavity diode laser with fixed direction output beam," *Review of Scientific Instruments*, vol. 72, pp. 4477–4479, December 2001.